CHAPTER I

Introduction

1.1.General introduction

Space physics is a new important major come into appearance in nowadays disciplines, just very recently because it is mainly concerned with our recent technology and devices dedicated for exploring our neighborhood planets and astronomical objects and the environment therein. Plasma physics considered as a core task in space physics and it has been addressed by many authors and they were trying to explain the phenomena encountered in such environment.

In this research the main task was addressed is the field line resonance (FLR) phenomenon. The FLR is generated when the frequency of a hydromagnetic wave in earth magnetosphere matches the eignfrequency of a geophysical field line. Field line resonance can be used to estimate plasma mass density.

Ultra Low Frequency (ULF) waves incident on the Earth are produced by processes in the magnetosphere and solar wind. These processes produce a wide variety of ULF wave types that are classified on the ground as either irregular pulsations (Pi) or continuous pulsations (Pc). Waves of different frequencies and polarizations originate in different regions of the magnetosphere. The location of the projections of these regions onto the Earth depends on the solar wind dynamic pressure and magnetic field. The occurrence of various waves depends on conditions in the solar wind and in the magnetosphere. Changes in orientation of the interplanetary magnetic field or an increase in solar wind velocity can have dramatic effects on the type of waves seen on the Earth. Similarly, the occurrence of a magnetospheric substorms or magnetic storms will affects which waves are to be seen. The properties of ULF waves seen at the ground contain information about the processes that generate them and the regions through which they have propagated. FLR is known to be one of the mechanisms to produce ULF. The study of ULF waves and FLR is a very active field in space research and much has yet to be learned about the processes that generate them.

Plasma is the name given to highly ionized gases; and in the magnetosphere plasma is threaded by a magnetic field. When the collision frequency in plasma is sufficiently low, the charged particles simply gyrate around the magnetic field and travel along it. Any force that moves the particles also moves the magnetic field and vise versa. In this situation the field and plasma are frozen together. This concept enabled Hannes

Alfven to describe a simple process that creates low frequency waves that propagates along a magnetic field lines. He received the Nobel Prize for this discovery and the waves he described are now called the Alfven waves, Alfven waves have a major role in the mechanism of FLR (Koskinen & Hannu, 2005).

1.2.Objectives of The Research

The purpose of this research is to use ground magnetic data at low latitude region to calculate a power spectrum and estimate the FLR frequency during an event of low latitude global mode ULF Pc 5(continuous pulsations), i.e.:

i. To check a single station (H/D) technique on determining FLR frequency from low latitude ground magnetic data.
ii. To justify the cavity/wave guide mechanism of the low latitude global mode pulsations.

1.3.Research Methodology

Time series of ground magnetic H-component and D-component data from a low latitude ground magnetometer (HERMANUS in South Africa) have been used in the analyses. The power spectrum of the filtered data in the period range: 10-1000 s was obtained and the H/D power spectrum curve is used to obtain the FLR frequency which is known as the single station method. In analyses some MATLAB codes were used and presented in the appendices.

1.4.Statement of The Research Problem

In situ devices such as satellites and other mission tools encounter with severe processes in the environment of the geospace; understanding space weather therefore is a very important task; many space weather processes took place in situ and may dramatically affect those devices and degrade them; among those processes is the enhancement of in situ electrons fluxes. ULF and other mechanisms have been known to play a major role in causing those enhancements, hence understanding all mechanisms and physics of the ULF's is very important.

1.5.Outline of The Research

In chapter I a general introduction including objectives and statement of the research has been presented; whence, chapter II covered an overview on space plasma; but all what

concerned with the FLR have been presented in chapter III. Finally: results, discussion and conclusion are all presented in chapter IV.

CHAPTER II

Space plasma

In this chapter we introduce general information about plasma: space plasma, solar wind and its components i.e. electrons and ions.

We also discussed the concept of geophysical plasma and the earth magnetosphere and ionosphere; whence we highlighted that plasmas are not only abundant in the universe, but also in our solar system.

2.1.Definition of a Plasma

Plasma is a gas of charged particles that consists of equal numbers of free positive and negative charge carriers; and having roughly the same number of charges with different signs in the same volume element guarantees that the plasma behaves quasi neutral in the stationary state. On average plasma looks electrically neutral to the outside, since the randomly distributed particle's electric charge fields mutually cancel each other. For a particle to be considered a free particle, its typical potential energy due to its nearest neighbor must be much smaller than its random kinetic (thermal) energy. Only then the particle's motion is practically free from the influence by other charged particles in its neighborhood as long as no direct collisions take place.

Since particles in plasma have to overcome the coupling with their neighbors, they must have thermal energies above some electron volts, thus typical plasma is a hot and highly ionized gas. While only a few natural plasmas, such as flames or lightning strokes, can be found near the Earth's surface, plasmas are abundant in the whole universe.

More than 99% of all known matter is in the plasma state (Baumjohann & Treumann, 1997). Plasma is quasi-neutral gas with so many free charges that collective electromagnetic phenomena are important to its physical behavior.

Quasi-neutrality means that in a given plasma element there is an equal amount of positive and negative charges. There is no clear threshold for the required degree of ionization. Roughly 0.1% ionization already makes the gas look like plasma, and 1% is sufficient for almost perfect conductivity (C.T.russell, 2003).

2.2.The Solar Wind Plasma

The temperature of the photosphere is less than 6000 K and as a result the sun is most luminous in what we call visible light. The temperature at first falls and then rises rapidly as one moves above the photosphere. This behavior is reminiscent of the behavior of the upper atmosphere of the Earth, in which the absorption of solar photons in the stratosphere and the thermosphere create warm layers well above the surface of the Earth. Here too the corona appears to be a region of heating from which heat is conducted downward to the chromospheres below and convicted outward from the corona by the solar wind. Understanding the source of this coronal heating is one of the outstanding problems of the solar wind.

The high temperature of the corona is important since the solar wind must escape the deep gravitational potential well of the sun. The escape velocity is 625 km/s from the surface of the sun. Thus a proton requires over 2 Kev to escape to infinity from the surface of the sun and about 0.5 Kev to escape from 5 Rs (Sun radius).

The Earth sits about 230 R s from the sun. The solar wind has achieved close to its asymptotic velocity by the time it reaches 1AU. For a coronal temperature of close to 106K the observed median solar wind velocity is obtained in this solution. Nevertheless, modeling the solar wind expansion is still an active area because we have few observational constraints on the nature of the "heating processes" in the acceleration region. In part because of the weakness of our understanding of the solar wind in those critical regions of the corona where we have not been able to obtain in situ data we concentrate in this review on solar wind phenomenology at 1AU.

The main components of the solar wind plasma are:

2.2.1. Electrons

Although, frequently it is possible to treat ions as a single fluid in the solar wind, but this is not true for electrons; since, electrons most frequently appear to have at least two components, a core and a halo, the core is colder than the halo and it is denser. It is important also to note that the thermal speeds of both populations are greater than the solar wind bulk speed. Thus the electrons can leave the sun much faster than the ions although in the direction perpendicular to the magnetic field they drift together at the same velocity. A paradox is introduced by this difference in velocity that arises because

in the corona the ions and electrons have similar temperatures but very dissimilar masses.

In a collision less gas, like the solar wind over most of its transit from the sun, charged particles do not leave their magnetic field lines. They also maintain quasi charge-neutrality. How can they do this if they are not traveling at the same speed? The answer is trivial if the source regions on the sun are constant in time so that the flux of electrons and ions at the base of a field line is constant. The density is always the same and it does not matter if the protons and ions stream relative to each other along the field.

If the solar wind production rate varies in time and the ion density along a flux tube varies with distance, then the electrons have to slow down as they pass through dense regions and then speed up in rarefied regions. This occurs because when there is an overabundance of ions there will be a polarization electric field that attracts the electrons to that region. In regions of under dense ions the electrons will be expelled by the excess negative charge. As a result, charge imbalances are minimal in the solar wind despite the speed differences and time variations. We might expect variations in the electric potential along the magnetic field but no detectable variation in charge neutrality. Because the core electrons travel most slowly they are affected the most by these electric potential variations, and the overall electric potential surrounding the sun.

2.2.2. Ions

Most solar wind instruments flown to date return counts versus energy per charge, which can be interpreted as counts per increment of velocity times the square root of mass/charge. In magnetized plasma the bulk velocity of all particles perpendicular to the field must be equal. The bulk velocity along the field need not to be so, and here it is clearly not equal. The reason for such differences must still be speculative, but since interpenetrating ion beams are not rare, it is important to understand their origin. The widths of these peaks are narrow compared to the energy of the peak. Thus the thermal velocity of the particles (the random component perpendicular to and parallel to the magnetic field) is small compared to the bulk velocity. This is an indication that they are supersonic. They move faster than the speed of a sound wave in the plasma. They also move faster than the magnetosonic velocity that is a combination of the sound and Alfven speeds. Not as obvious here is the fact that the alpha particles have temperatures about four times greater than those of the protons.

In fact all ions have temperatures that on average are roughly proportional to their atomic mass, i.e. their thermal velocities are roughly equal. This relationship, however, is not strictly obeyed**.**

Coulomb collisions tend to equilibrate these temperatures, especially when the ion temperatures are low. Thus deviations from this relation are found in cool dense solar wind flows and $\boldsymbol{He^{++}}$cools more rapidly with heliocentric radius than protons **(B.Roberts, 2001)**.

2.3.Geophysical Plasmas

Plasmas are not only abundant in the universe, but also in our solar system. Even in the immediate neighborhood of the Earth, all matter above about 100 km altitude, within and above the ionosphere, has to be treated using plasma physical methods. There are quite a number of different geophysical plasmas, with a wide spread in their characteristic parameters like density and temperature.

2.4.Magnetosphere

The shocked solar wind plasma in the magnetosheath cannot easily penetrate the terrestrial magnetic field but is mostly deflected around it. This is a consequence of the fact that the interplanetary magnetic field lines cannot penetrate the terrestrial field lines and that the solar wind particles cannot leave the interplanetary field lines due to the aforementioned frozen-in characteristic of highly conducting plasma.

The boundary separating the two different regions is called magnetopause and the cavity generated by the terrestrial field has been named magnetosphere**.**

The kinetic pressure of the solar wind plasma distorts the outer part of the terrestrial dipolar field. At the front side it compresses the field, while the night side magnetic field is stretched out into a long magnetotail which reaches far beyond lunar orbit.

The plasma in the magnetosphere consists mainly of electrons and protons. The sources of these particles are the solar wind and the terrestrial ionosphere. In addition there are small fractions of $He^{+}$and O^{+}ions of ionospheric origin and some He^{++}ions originating from the solar wind. However, the plasma inside the magnetosphere is not evenly distributed, but is grouped into different regions with quite different densities and temperatures.

The radiation belt lies on dipolar field lines between about 2 and **6** $\boldsymbol{R_E}$(1 Earth radius = 6371 km). It consists of energetic electrons and ions which move along the field lines and oscillate back and forth between the two hemispheres. The magnetic field strength ranges between about 100 and 1000 n T (Baumjohann & Treumann, 1997).

Most of the magnetotail plasma is concentrated around the tail mid plane in an about 10 $R_E$thick plasma sheet. Near the Earth, it reaches down to the high-latitude auroral ionosphere along the field lines. The outer part of the magnetotail is called the magnetotail lobe. It contains a highly rarified plasma with typical values for the electron density and temperature and the magnetic field strength, $B \approx 30\, n\, T$.

Down here, we show in Figure 2.1 an artificial view representing the Earth's magnetosphere with its different plasma population regions.

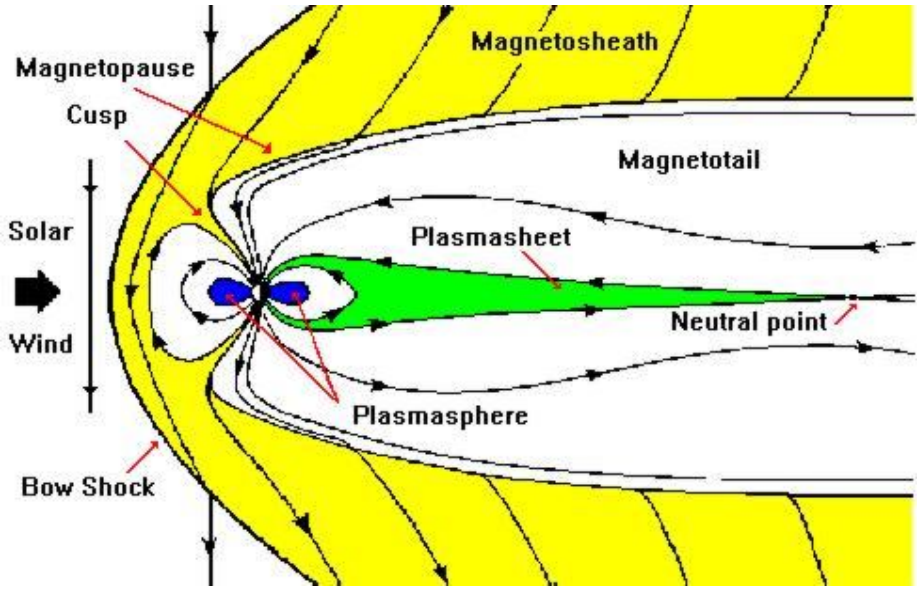

Figure 2.1 Plasma population in Earth's magnetosphere, (Christian, 2013)

2.5.Ionosphere

The solar ultraviolet light impinging on the Earth's atmosphere ionizes a fraction of the neutral atmosphere. At altitudes above 80 km collisions are too infrequent result in rapid recombination but with the production source, i.e. the ultraviolet radiation from the sun a permanent ionized population called the ionosphere is formed. The ionosphere

extends to rather high altitudes and at low- and mid-latitudes gradually it merges into the plasmasphere.

The plasmasphere is a torus shaped volume inside the radiation belt. It contains cool but dense plasma of ionospheric source. In the equatorial plane, the plasmasphere extends out to about 4 R_E(earth radius). At high latitudes plasma sheet electrons can precipitate along magnetic field lines down to ionospheric altitudes, where they collide with and ionize neutral atmosphere particles. As by-product, photons emitted by this process create the polar light, the ***au***rora. These auroras are typically observed inside the auroral oval**,** which contains the footprints of those field lines which thread the plasma sheet. Inside of the auroral oval lies the polar cap, which is threaded by field lines connected to the tail lobe (Baumjohann & Treumann, 1997).

2.6.Magnetohydrodynamic Waves

Magnetohydrodynamic waves are found in a wide variety of astrophysical plasmas. They have been measured in plasma fusion devices and detected in the magnetosphere of earth, the solar wind and a number of magnetic structures seen in the Sun's atmosphere; in space plasmas their detection is often indirect, by matching measured properties (such as propagation speed or pressure variation) with theoretically deduced properties and correlations, although the magnetosphere and solar wind provide direct *in situ* measurements of those waves.

A complication in the identification of magnetohydrodynamic waves in space plasmas has been the realization that generally such plasmas are strongly inhomogeneous, structured by magnetism, plasma density and temperature variations, or by plasma flows. This strong inhomogeneity brings about complications in the description of magnetohydrodynamic wave phenomena, with magnetic flux tubes and plasma flow tubes being of special interest. In the solar atmosphere, sunspots, solar photospheric magnetic flux tubes, coronal loops and polar plumes are examples of flux tube structure and oscillatory phenomena have been detected in all of them. Oscillations have also been detected in solar prominences and generated by solar flares. Waves are the way in which information in a medium may be communicated from one region to another. In a gas communication can be achieved by sound waves, in the form of compressions and rarefactions of the medium which propagate at the sound speed C_s (B.Roberts, 2001)**.**

2.7.Alfven waves

The concept of Alfven wave is very important when we need to deal with space plasma and the geomagnetic field.

In Alfven model to derive a generation of an Alfven wave considere an infinite volume of fully ionized hydrogen, imagine that a force is applied to the slab of plasma perpendicular to the magnetic field flux density **B** displacing a rectangular section of plasma with velocity **V**. As the charges being to move they experience Lorentz force $F = q(V \times B)$ where q is the charge in Coulombs. The electrons move to the left side of the moving slab, and the protons to right side. This polarization of the charges creates and electric field **E** orthogonal to both **V** and **B.**

If the slab were in a vacuum the force of the electric field would eventually stop any further transfer of charge. At this point the electric force would be equal and opposite to Lorentz force so that $\boldsymbol{E = -V \times B}$**.** However in a plasma the charge can flow through the surrounding fluid in an attempt to neutralize the polarization. This charge motion creates an electrical current density **J**. As this current flows across the magnetic field above and below the moving slab it exerts a force on the gas $\boldsymbol{F = J \times B}$**,** this force is in the same direction as the initial motion of the slab. Consequently, the plasma above and below begins to move.

The initial disturbance is propagating in both directions along the magnetic field away from the initial disturbance. The displacement of the plasma slab distorts the magnetic field that is frozen into the plasma. As the field bends, tension develops creating a restoring force that brings the slab to a stope and then returns it towards its initial location. As this happens the moving slabs above and below the initial slab distort the field line in the same way so that to pulses appear to propagate away of the origin. These pulses are Alfven waves. (L & McPherron, 2003)

2.8.The Geomagnetic Field

The first clear description of the geomagnetic field was by William Gilbert in 1600, through a series of experiments that showed that Earth is magnetized and possesses magnetic poles. By now we know that the total strength of this field is around 0.066 mT near the poles and 0.024 mT near the equator. By comparison a small bar

magnet produces a field of order 10 mT. Note that Tesla, T, is actually the unit of magnetic flux density or magnetic induction B, The needle of a magnetic compass points at an angle to true (geographic) north.

From figure (2.2), angle of deviation is called the magnetic declination (positive when east of true north) and varies with location, as reported by Christopher Columbus in 1492. The first declination chart of Earth was produced by Edmund Halley (1702). At low latitudes, the declination is typically a few degrees, but may approach 90º in the polar region. For example, at Davis station in Antarctica, the declination in January 2010was 79º29´ The geomagnetic field vector F is usually described in terms of total field intensity F, the horizontal intensity H (in n T), the inclination (or dip angle) I of F with respect to the horizontal plane, and the declination D (in degrees). At Davis in Antarctica, I=71º59´, and F=54459 n T, as of January 2010. Note that in practice, H is often used to describe the magnetic field.

An orthogonal X, Y, Z coordinate system (representing field intensity in the north, east, and vertical directions) is also widely used, especially at high latitudes. The relationship between these coordinates is illustrated in Figure 2.2. We see that $H = \mathbf{F \cos I}, \mathbf{Z = F \sin I}, \mathbf{X = H \cos D \text{ and } Y = H \sin D}$ (2.1)

Were **F** is the total field intensity, **I** is the inclination (or dip angle), **H** is the horizontal intensity (in n T), **D** is the declination (in degrees).

The geomagnetic field measured at the surface of Earth includes contributions from sources within Earth's core, the crust and upper mantle, and a disturbance field representing electric currents flowing in the ionized part of the atmosphere (the ionosphere) and in the magnetosphere (Menk & Waters, 2013).

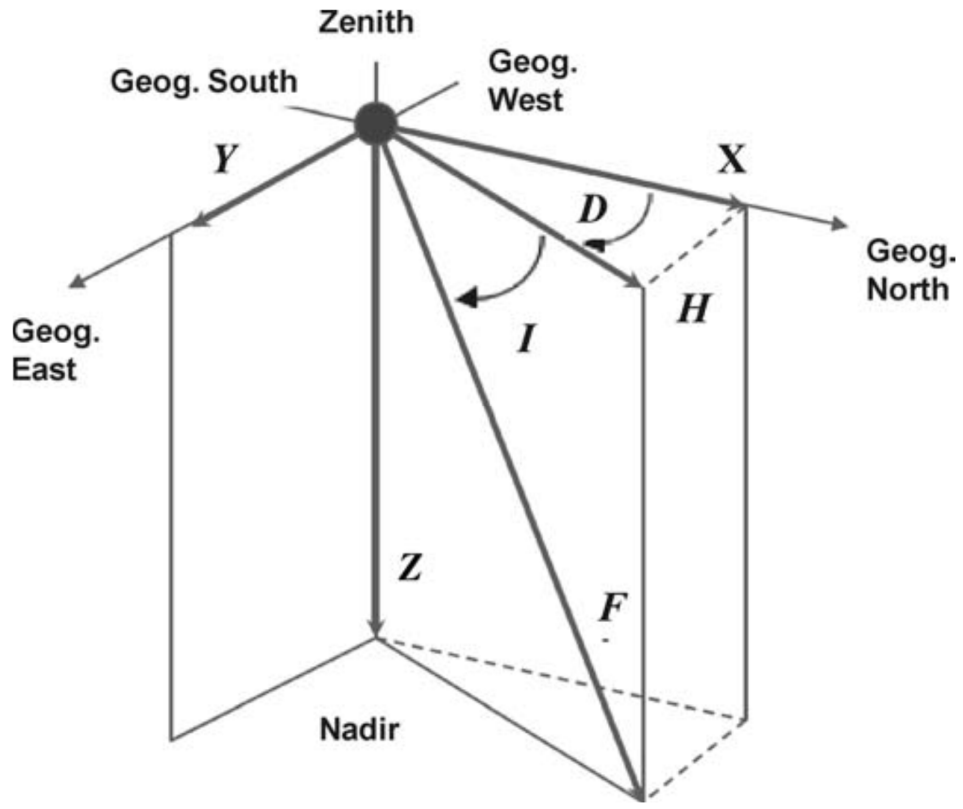

Figure 2.2 Components of the geomagnetic field, where $H = F\,cosI, Z = F\,sinI, X$ =H cos D, Y=H sin D, and $F = \sqrt{x^2 + y^2 + z^2} = \sqrt{H^2 + z^2}$ (Menk & Waters, 2013)

The core field is produced by self-exciting dynamo action due to differential rotation between the inner and outer regions of the conducting outer core of Earth. The resultant field is approximately dipolar and the axis of this centered dipole is tilted by about 10º with respect to Earth's geographic rotation axis. Such a dipole accounts for about 90% of the geomagnetic field at the surface. The core field changes slowly with time, called secular variation, and includes large-scale anomalies associated with eddy circulations in the outer core.

The crustal field arises from relatively small-scale sources of induced or remnant magnetization of rock and may significantly affect local magnetic measurements. This field varies widely with location and is mapped with ground-based, marine, aeromagnetic, and high-precision satellite surveys. Such surveys provide vital information to the geophysics exploration community that is concerned with locating and exploiting mineral deposits. The disturbance field due to external sources varies with location and time and is of particular interest. We will discuss it in more detail later. The dipole axis cuts Earth's surface at the geomagnetic poles. VOSTOK station in Antarctica

is located near the south geomagnetic pole, which at epoch 2010 was at 80º02´S, 107º8´E. Strictly speaking, this is a north pole since it attracts the south pole of magnets. The regions of peak auroral activity, the auroral ovals, are approximately centered on the geomagnetic poles. The positions of the actual magnetic poles, where a compass needle stands vertically, depend on local effects in the crust and do not coincide with the geomagnetic poles. Determining the locations of these poles was an important goal for early explorers. At epoch 2010, the north magnetic pole was located at 84º97'N, 132°35`W and the south magnetic pole at 64°42`S, 137°34`E. When Edgeworth David Mawson, and Mackay reached the south magnetic pole on January16, 1909, it was located at 71°36'S, 152°0'E.

The magnetic field due to a centered dipole is represented in spherical coordinates by

$$Br = -\frac{M}{r^3} 2cos\theta$$

$$B\theta = -\frac{M}{r^3} \sin\theta \qquad (2.2)$$

$$B\phi = 0$$

Were θ is colatitude ,ϕ is the latitude ,($Br, B\theta, B\phi$)are the magnetic field intensity in the spherical coordinates

The total intensity is given by

$$B = -\frac{M}{r^3}[3cos\theta + 1]^{1/2} \qquad (2.3)$$

r is geocentric distance

where r is measured from the center of Earth and θ is the colatitude measured from the dipole axis. M=7.8x10^{22}AM^2 is the dipole moment of Earth. This has been decreasing. The equation that describing a dipole field line is then given by

$$r = r_o \, sin^2\theta \qquad (2.4)$$

where r_o is the geocentric distance at which the field line crosses the equator.

The magnetic shell parameter L is commonly used to describe the equivalent distance in R_E(earth radius)by which dipole field lines extend into space at the equator, mapping out magnetic shells with $LR_E = r_o$.

A centered dipole is a poor approximation to the actual field. An improvement is gained by using an eccentric axis dipole, based on a tilted dipole source displaced about 560km from Earth's center, toward the Mariana Islands, east of the Philippines. (Menk & Waters, 2013)

2.9.Previous Studies

Here, we have selected two studies carried out previously addressing the issue of estimating FLR and highlighted their findings.

2.9.1. Simultaneous observations of the plasma density on the same field line by the CPMN ground magnetometers and the Cluster satellites (Maeda, et al., 2008)

In this study by (Maeda, et al., 2008), applied cross-phase method and the amplitude-ratio method to magnetic field data obtained from two ground stations located close to each other, they determined the frequency of the field line resonance (FLR), or the field line eigenfrequency, for the field line running through the midpoint of the two stations. From thus identified FLR frequency they estimated the equatorial plasma mass density. Their findings are:

They identified 19 events in which the Cluster spacecraft were located on the field line running through the midpoint of Tixie (TIK) and Chokurdakh (CHD) stations when they observed FLR, and statistically compared the simultaneously observed plasma mass density (ρ) and electron number density (Ne), although the number of events are limited (19). they identified the FLR frequency at about 4 m H z.

2.9.2. Computing magnetospheric mass density from field line resonances in a realistic magnetic field geometry (Berube, et al., 2006)

Here in their study (Berube, et al., 2006) they focused on using Ultra-low-frequency (ULF) field line resonances to infer the mass density along magnetospheric magnetic field lines. They investigated the importance of including a realistic magnetic field geometry that is when computing plasma mass density from observed field line frequencies. Their findings are:

They investigated the importance of choosing realistic magnetic field geometry in relation to the problem of determining the mass density along magnetic field lines from observed field line resonance frequencies. They have shown that the extent to which field line eigenfrequencies depend on field line geometry is significant.

CHAPTER III

Field line resonance

In this chapter we discussed in some details the concept of field line resonance which is generated when the frequency of hydromagnetic waves matches the eignfrequency of a geophysical field line. Determining FLR frequency is very important because we use it to estimate plasma mass density (numerically).

3.1.Field line resonances

Field lines of the Earth's dipole behave like vibrating strings as illustrated in Figure 3-1. The ends of the field lines are frozen in the conducting ionosphere and can't move although they can bend. In their equilibrium positions there is no force orthogonal to the lines. However, if some process displaces a field line, a tension force develops that tries to restore it to its equilibrium shape. However, because the field line is loaded with gyrating particles it picks up momentum that causes it to overshoot the equilibrium. The field line thus oscillates until other processes damp it.

There are two primary modes of oscillation of a dipole field line. The toroidal mode is a displacement in the azimuthal direction creating an azimuthal magnetic perturbation as shown in the right panels of Figure3.1; the poloidal mode is a radial displacement with radial magnetic perturbations as shown in the middle panels. Either mode may oscillate with different harmonics. The fundamental harmonic depicted in the top row contains an odd number (one) of half wavelengths between the ends of a field line. The second harmonic in the bottom row contains an even number (2) of half wavelengths. Many different harmonics may be simultaneously excited when the field line is excited by a broadband source (Sciffer & Waters, 2008).

The toroidal mode of field line resonances is most commonly observed in space. The reason is that azimuthal perturbations do not change the field magnitude or cause plasma density changes. In addition, field lines azimuthally adjacent to the vibrating line have nearly the same resonant frequency and so can vibrate in phase with the initially disturbed line. In fact, these properties identify this mode as the Alfven wave.

The Poloidal mode is harder to excite because field lines are oscillating in a radial direction and radially adjacent field lines have different frequencies. Inevitably, adjacent field lines will oscillate out of phase and there will be compressions and rarefactions of

the field. This mode of field line resonance corresponds to the fast mode (Sciffer & Waters, 2008).

The simplest approximation to the fundamental frequency of a field line is obtained by integrating the Alfven travel delay $d\,t\, =\, ds/V_A$ along the field line. The local delay depends on both the field strength and the plasma density through V_A. Longer field lines have longer resonant periods (lower frequencies). Field lines with more, or heavier particles will also have longer periods. The sudden decrease in velocity and frequency at about five R_E is caused by the increase in plasma density across the plasmapause. The decrease close to the ionosphere is caused by the presence of oxygen ions in the upper ionosphere. The slow increase in resonant frequency from 3 m Hz at the magnetopause to 20 m Hz at the plasmapause, and a much larger increase inside the plasmapause are caused mainly by a rapid increase in field strength and a decrease in field line length.

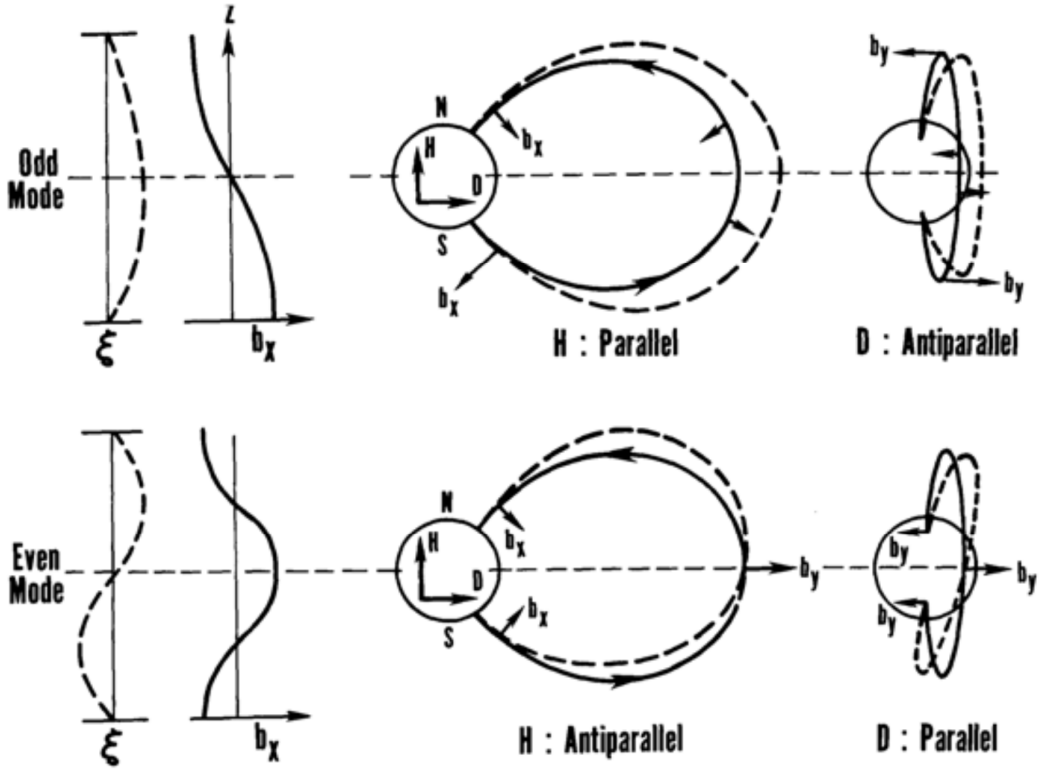

Figure3.1: The field lines of a dipole (middle panels) may be approximated as stretched strings (left panels). The dipole lines may be displaced and oscillate in two

orthogonal directions – radial (center panels) and azimuthal (right panels) (Sciffer & Waters, 2008)**.**

Any process that displaces a field line can excite field line resonances.

The most common source is ULF waves propagating through the magnetosphere after having been transmitted through the magnetopause. Another source is waves created at the magnetopause that are evanescent inside the magnetosphere (spatially damped). A third source is sudden changes in magnetospheric plasma flow velocity such as those that occur in substorms (Sciffer & Waters, 2008).

3.2.Techniques for Detecting Field Line Resonances

The experimental detection of FLRs began in the late 1950s where the effect was considered analogous to a stretched string resonance, The string tension, mass per unit length and string length are associated with the magnetic field tension, plasma mass density and the distance along the field between conjugate ionospheres. The plasma mass density is distributed along the magnetic field in the magnetosphere in a non uniform manner. Therefore, the variation of the wave fields along the magnetic field line is not sinusoidal like the uniform-density, stretched string case. The eigenfunction that describes a "natural mode" of the system depends on the variation of the Alfven velocity, which for field lines greater than $L \sim 1.5$ usually has a minimum in the equatorial plane, (Waters, et al., 2006)

There are many types of techniques to determine FLR as:

3.2.1. Variation in Spectral Power with Latitude

The variation of the Alfven speed in the magnetosphere leads to an increase in the FLR frequency with decreasing radial distance except across the plasmapause region and at very low latitudes (L<1.4). For shear Alfven FLRs that have largely an azimuthal (b) magnetic perturbation in space, transition through the ionosphere rotates the field vector by 90°.

Therefore, if FLRs have sufficient amplitude, they may be identified in the power spectra of data obtained from the magnetometer time series from a north–south-oriented sensor.

The process begins with an examination of the baseline removed, magnetic field time series from the north–south (x-component) sensors of a collection of stations that are located at different latitudes but at similar longitudes. For intervals that show ULF wave

activity, the data are transformed into the frequency domain. We identify these spectra by X(f) and Y(f) for data obtained from the north–south [x(t)] and east–west [y(t)] magnetometer sensor time series, respectively.

The common method is to use the FFT (Fast Fourier Transform). However, the maximum entropy method (MEM) and wavelet and Hilbert transforms have also been applied. The FFTs of the time series segments are then represented as a stack plot of spectral amplitude or power density versus frequency.

Additional resonance information, such as the phase, is therefore often included to improve FLR identification.

3.2.2. Variation of Phase with Latitude

Waves contain both amplitude and phase information. As with other wave types, the phase properties of ULF waves also provide a rich source of information, a fact that was used in early attempts to use wave polarization information to identify FLRs.

There are several ways in which the phase information may be used to identify FLRs. The first process is similar to the spectral power with latitude already discussed:

(i) Obtain ULF wave time series data from a latitudinal distribution of sensors (e.g., magnetometers, photometers, and HF radar beam).

(ii) For a given time interval, calculate the FFT of these data.

(iii) Plot the phase as a function of latitude for a given frequency.

The phase data are usually combined with the spectral amplitude with latitude.

3.2.3. Spectral Power Difference and Division

These methods are identified as the “gradient” method in the literature, and depend on magnetic field measurements of the ULF fields at closely spaced, latitudinal sites. The required latitudinal magnetometer separation depends on the quality of the resonance and the variation of FLRs with latitude, which is directly related to the radial variation of the Alfven speed in the magnetosphere. Essentially, we need to obtain sufficient difference in FLR frequency at the two sites while keeping the stations close enough to ensure coherent signals. For $L<2.8$, site separations of 80km have been successfully used while at higher latitudes ($L>5$), separations of the order of 200km have been used.

The process first requires that a suitable time interval of magnetometer data from two latitudinally separated, north–south oriented sensors is transformed into the frequency domain, usually by the FFT and the researcher's preferred windowing function.
We denote these as the equatorial and poleward spectra (XE (f) and XP (f)) These amplitude or power spectra are then either subtracted or divided and plotted as a function of frequency.

3.3.Single Station H/D

FLR signatures measured on the ground have small azimuthal wave numbers since the smaller spatial scale perturbations attenuate in amplitude from the ionosphere to the ground. This selects those FLRs in the magnetosphere that have a predominantly azimuthal (east–west; y) variation in the perturbation magnetic field. In the magnetosphere, the FLR exhibits properties of the shear Alfven wave mode where the perturbation magnetic field(b) and the associated field-aligned current are related by $\nabla \times b = \mu j$. However, in the atmosphere, $\nabla \times b = 0$, which implies a rotation of the perturbation magnetic field (b) in the north–south (x) direction for detection by ground magnetometers. If the x component magnetometer sensor data contain the FLR signal and the y-sensor data are dominated by the source spectrum, then a two-sensor, horizontal and orthogonal arrangement should be suitable for FLR detection.

A method that has been used is to calculate the spectral power using data from the two orthogonal sensors and plot the ratio $X(f)/Y(f)$. This is also known as the H/D technique. The x-component spectra should peak at the FLR frequency.

There was some improvement in the FLR signature at the lower latitudes as the y-component spectrum $Y(f)$ has a normalizing effect on the x-component data. However, $Y(f)$ is not necessarily flat and depending on the variation of power with frequency in the y-component data, the FLR frequency identified by $X(f)/Y(f)$ may be shifted to lower or higher frequencies. Single station power ratio measurements can be use successfulness.

A driven harmonic oscillator passes through a phase difference of 90° at resonance between the resonance oscillation and the driver term. Therefore, a cross phase analysis using the X (f) & Y (f) spectra may yield the FLR where the phase difference is 90° (Menk & Waters, 2013).

CHAPTER IV

Results, Discussion, Conclusion and Recommendation

In this chapter the FLR frequency was estimated from the power spectrum graphs of the H (geomagnetic component) data and D (geomagnetic component) data. We present a discussion afterwards and finally we made some recommendation and conclusion.

4.1.Results

In the following Figure4.1 the power spectrum of the H component data has been calculated, the time span of the data is 48 hours (3 and 4 hours UT) on the day of: September 4, 2009, data were collected from 'HER' station that belong to the Magnetic Data Acquisition System ($MAGDAS$) chain of magnetometers (Yoshikawa, 2017), and during these hours a global low latitude mode Pc 5 pulsations were recorded, for more information on criteria to extract the global mode see (Suliman, et al., 2013).

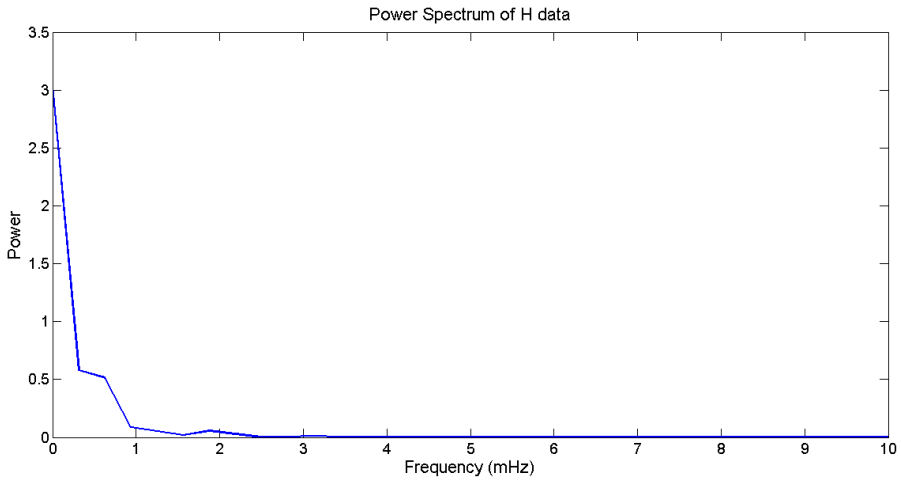

Figure4.1 Power spectrum of the filtered H component ($1 - 100\ mHz$) observed at HERMANUS magnetometer station from 3-4 hours UT on September 4, 2009, it show small peak in frequency around 2 m Hz.

Using time series D (geomagnetic component) data obtained from the same station in the same period span: 3-4 hours UT on September 4, 2009, the power spectrum was calculated and shown here in following Figure4.2

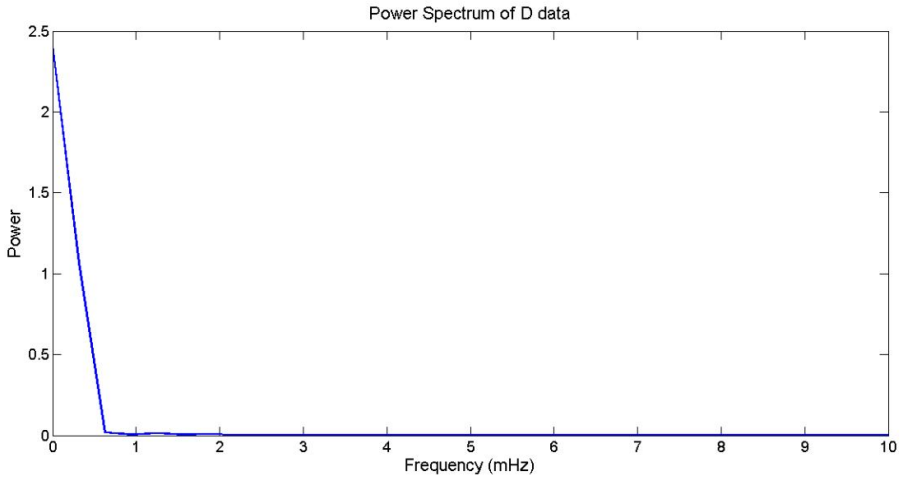

Figure4.2 Power spectrum of the filtered D component (1-100 m Hz) observed at HERMANUS magnetometer station from 3-4 hours UT on September 4, 2009.

And in order to estimate the (FLR) frequency, we plot H/D power spectrum and from the graph we obtained an FLR resonance, i.e. $2.5\,mHz$ which is indicated by the red dot in Figure4.3

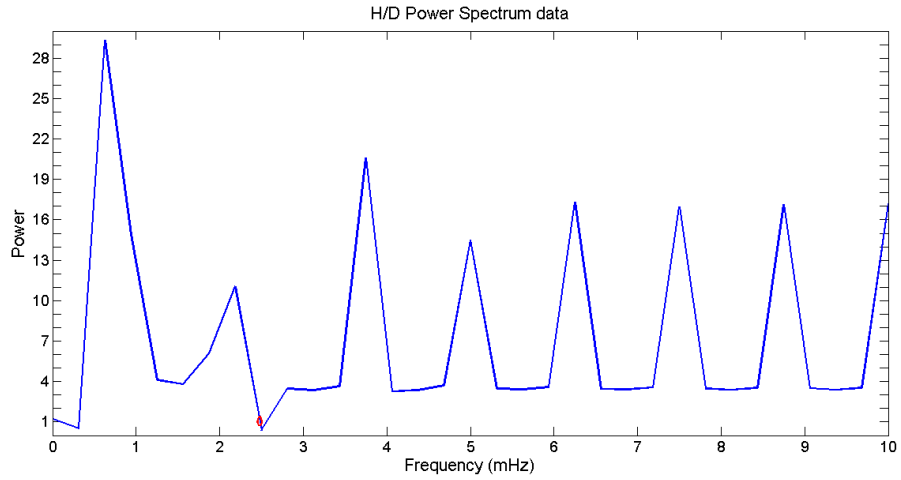

Figure4.3 The H\D power spectrum, the red dot shows the (FLR) frequency.

4.2.Discussion

The ground H component magnetometer data contained the FLR signal and the D component data are dominated by the source spectrum in the geospace, then the FLR frequency is found in the peak of H component power spectrum. To estimate the FLR we plot H/D power spectrum and we obtained the frequency in the peak of the H/D spectrum which correspond to unity in vertical axis contains the H/D power spectrum data. Accordingly, the obtained FLR frequency was found to be $2.5\ mHz$.
Moreover, the feature of the field line resonance FLR is hard to be seen in our data, and this is because the station from which data are collected lay in closer low latitudes in the magnetic model of the Earth.

There exist more than one technique to deduce field line resonance (FLR) frequency, but the single station technique is direct to be used and gave obvious and reasonable result here regarding the estimation of the FLR frequency.

4.3.Conclusion

We observed and obtained the field line resonance frequency, it was found to be equal $(2.5\ m\ hz)$.

Near Earth space weather is tremendously important in terms of plasma mass density available there; therefore, estimation of plasma mass density through knowledge of FLR is valuable in the space weather and researchers are still addressing this problem.

4.4.Recommendation

Because the field line resonance frequency FLR can be used in estimation of the plasma mass density via numerical methods; we recommend that to continue the task of this research problem and try next to estimate the plasma mass density using the FLR frequency obtained during onset of global mode Pc 5 pulsations.

References

B.Roberts, 2001. Magnetohydrodynamic Waves. *E NCYCLOPEDIA OF ASTRONOMY AND ASTROPHYSICS,* 29 1, BS1 6BE(785998), p. 6.

Baumjohann, W. & Treumann, R. A., 1997. *BASIC SPACE PLASMA PHYSICS.* fiest ed. london: Imperial College Press.

Berube, D., Moldwin, M. B. & Ahn, M., 2006. Computing magnetospheric mass density from field line resonances in. *JOURNAL OF GEOPHYSICAL RESEARCH,* 111, A08206,(10.1029/2005JA011450), p. 7.

C.T.russell, 2003. *solar wind and inter planetary magnetic field,* los angles: University of California,.

Christian, D. E. R., 2013. *COSMICOPIA.* [Online]
Available at: https://helios.gsfc.nasa.gov/magnet.html
[Accessed 19 2 2017].

Koskinen & Hannu, 2005. *Lectures in Advanced Space Physics,* london: Rami Vainio.

L, R. & McPherron, 2003. magnetic polsation ;ther sourses and relation to solar wind. *Geophysics and Planetary Physics,* CA 90095(1567), p. 32.

Maeda, N., Takasaki, S., Kawano, H. & Ohtani, S., 2008. Simultaneous observations of the plasma density on the same field. *science direct,* 04.016(0273-1177), p. 8.

Menk, F. W. & Waters, C. L., 2013. *Magnetoseismology.* first ed. Weinheim, Germany: Wiley-VCH Verlag & Co. KGaA, Boschstr.

Sciffer, M. D. & Waters, C. l., 2008. field line resonance frequencies and spherical conductance. *joprnal of geophysical research,* 113(,A05219), p. 12.

Suliman, M. E. Y. et al., 2013. *The Relation Between Amplitudes of a Global-Mode Pc 5 Pulsations and Geosynchronous Electron Fluxes.* Melaka, IEEE.

Waters, C. et al., 2006. Remote Sensing the Magnetosphere Using Ground-Based. *Geophysical Monograph,* 169(0.1029/169GM21), p. 22.

Yoshikawa, A., 2017. *International Center for Space Weather Science and Education.* [Online]
Available at: http://www.serc.kyushu-u.ac.jp/index.html
[Accessed 15 02 2017].

Appendix A

MATLAB code to calculate and plot power spectrum of (D) and (H) components at HER station

```
[MagData,Header,STATDATA,CORRECT_INF]=read_1M('C:\Users\ICSWSE\De
sktop\MAGDAS1\HER\MIN\2009\HER_MIN_200909040000.MGD');
Hdata=MagData(:,1);
Ddata=MagData(:,2);
%plot(Hdata)
%figure;
%plot(Ddata)
day2Hdata=Hdata(49:96);
day2Ddata=Ddata(49:96);
%plot(day2Hdata)
%figure;
%|plot(day2Ddata)
Fs = 0.02;            % Sampling frequency
t = 0:1/Fs:1;         % Time vector
x = day2Hdata;  % 200 Hz sinusoid signal
nfft = 2^(nextpow2(length(x)));   % Find next power of 2
fftx = fft(x,nfft);
NumUniquePts = ceil((nfft+1)/2);
fftx = fftx(1:NumUniquePts);
mx = abs(fftx);
mx = mx/length(x);
mx = mx.^2;
if rem(nfft, 2)   % Odd nfft excludes Nyquist
  mx(2:end) = mx(2:end)*2;
else
  mx(2:end -1) = mx(2:end -1)*2;
end
f = (0:NumUniquePts-1)*Fs/nfft;
plot(f,mx);
title('Power Spectrum of H data');
xlabel('Frequency (Hz)');
ylabel('Power');


function [MagData,Header,STATDATA,CORRECT_INF]=read_1M(FileName)


%=============================================================
============
%
%   [MagData,Header,STATDATA,CORRECT_INF]=read_1M(FileName)
%
%   Read 1-Minute data of MAGDAS staraged data
%
%   Input: FileName
%   Outout: MagData     : Magnetic Data
[H,D,Z,F,Inc_EW,Inc_NS,Temp] (1440x7/1day)
%           Header      : Header Information (Structure array)
```

```
%           STATDATA    : Status Data of the Magnetometer
(Structure Array)
%           CORRECT_INF : GPS Time Correct Information (Structure
Array)
%
%   2003/10/09    Ver. 1.0 by K. Kitamura
%   2004/07/22    Ver. 1.1
(ŽžZ?³‰ñ?”,âƒwƒbƒ_?[,ÌŒJ,è•Ô,µ,O,É‘Î‰ž?j
%=============================================================
============

%clear all
%FileName=('S20030820.KUJ')

%=================  Open file ===================

[Fid,Message]=fopen(FileName,'r','l');

if Fid<0,
    disp(Message)
    return
end

% ============== Find magnetic data ======================

ReadUnit=1000;      FindMag=0;  NumRead=0;
Status=fseek(Fid,0,'bof');

while FindMag==0,

    [Buff,Count]=fread(Fid,ReadUnit,'uchar');
    [Message,Errnum]=ferror(Fid);
    if Errnum~=0,
        error(Message)
    end
    NumRead=NumRead+1;

    Find1A=find((Buff-26)==0);
    if length(Find1A)>0,
        for i=1:length(Find1A),
            if Find1A(i)~=ReadUnit,
                if Buff(Find1A(i)+1)==0,
                    MagPos=(NumRead-1)*ReadUnit+Find1A(i)+1;
                    FindMag=1;  break;
                end
            else
                [Buff,Count]=fread(Fid,ReadUnit,'uchar');
                [Message,Errnum]=ferror(Fid);
                if Errnum~=0,
                    error(Message)
                end
                NumRead=NumRead+1;
                if Buff(1)==0,
                    MagPos=(NumRead-1)*ReadUnit+1;
                    FindMag=1;  break;
                end
            end
```

```
        end
    end
end

fclose(Fid);
% ============== Read header ============================
[Fid,Message]=fopen(FileName,'rt');

if Fid<0,
    disp(Message)
    return
end

Status=fseek(Fid,0,'bof');

    head=fgetl(Fid);
    Header.DATA_TYPE=sscanf(head(10:end),'%s');
    head=fgetl(Fid);
    Header.SERIAL_NUM=str2num(head(11:end));
    head=fgetl(Fid);
    Header.STATION_NAME=sscanf(head(13:end),'%s');
    head=fgetl(Fid);
    Header.GEODETIC_LATITUDE=str2num(head(18:end));
    head=fgetl(Fid);
    Header.GEODETIC_LONGITUDE=str2num(head(19:end));
    head=fgetl(Fid);
    Header.RECORD_TIME=sscanf(head(12:end),'%s');
    head=fgetl(Fid);
    Header.REPORTED=sscanf(head(9:end),'%s');
    head=fgetl(Fid);
    Header.SAMPLING_TIME=str2num(head(14:end));
    head=fgetl(Fid);
    Header.MAG_RANGE=str2num(head(10:end));
    head=fgetl(Fid);
    Header.HEADER_DATA_NUM=str2num(head(18:end));

    if Header.HEADER_DATA_NUM~=0
        for i=1:Header.HEADER_DATA_NUM
                head=fgetl(Fid);

STATDATA(i).HEADER_DATA_TIME=sscanf(head(17:end),'%s');
                head=fgetl(Fid);
                STATDATA(i).BAIAS_H=str2num(head(8:end));
                head=fgetl(Fid);
                STATDATA(i).BAIAS_D=str2num(head(8:end));
                head=fgetl(Fid);
                STATDATA(i).BAIAS_Z=str2num(head(8:end));
                head=fgetl(Fid);
                STATDATA(i).BAIAS_F=str2num(head(8:end));
        end
    else
            STATDATA=[];
    end

    head=fgetl(Fid);
    Header.CORRECT_NUM=str2num(head(12:end));
```

```
    if Header.CORRECT_NUM~=0
        for i=1:Header.CORRECT_NUM
                head=fgetl(Fid);
                CORRECT_tmp=sscanf(head(12:end),'%s');
                CORRECT_INF(i).TIME=CORRECT_tmp(1:8);

CORRECT_INF(i).VALUE=str2num(CORRECT_tmp(10:end));
        end
    else
        CORRECT_INF=[];
    end
fclose(Fid);


% HEADER{1}=Header;
% HEADER{2}=STATDATA;
% HEADER{3}=CORRECT_INF;

%=================  Read Data ====================

[Fid,Message]=fopen(FileName,'r','l');
    % ============== Calculate size of magnetic data =========

    Status=fseek(Fid,0,'eof');
    EOFid=ftell(Fid);
    DataSize=EOFid-MagPos;

    %=======================================
    Status=fseek(Fid,MagPos,'bof');
    [MagData,Count]=fread(Fid,[7,DataSize/28],'float32');

    %========== convert error data (NaN) to
99999.99=================
    [errorrow,errorcol]=find(isnan(MagData)==1);
    MagData(errorrow,errorcol)=999999.9;
    MagData=MagData';
fclose(Fid);
```

Appendix B

MATLAB code to calculate and plot (H/D) at HER station

```
Fs = 0.02;            % Sampling frequency
t1 = 0:1/Fs:1;         % Time vector
x1 = day2Hdata;  % 200 Hz sinusoid signal
nfft1 = 2^(nextpow2(length(x1)));   % Find next power of 2
fftx1 = fft(x1,nfft1);
NumUniquePts1 = ceil((nfft1+1)/2);
fftx1 = fftx1(1:NumUniquePts1);
mx1 = abs(fftx1);
mx1 = mx1/length(x1);
mx1 = mx1.^2;
if rem(nfft1, 2)   % Odd nfft excludes Nyquist
mx1(2:end) = mx1(2:end)*2;
else
  mx1(2:end -1) = mx1(2:end -1)*2;
end
f1 = ((0:NumUniquePts-1)*Fs/nfft)*1000;
%Fs = 0.02;            % Sampling frequency
t2 = 0:1/Fs:1;         % Time vector
x2 = day2Ddata;  % 200 Hz sinusoid signal
nfft2 = 2^(nextpow2(length(x2)));   % Find next power of 2
fftx2 = fft(x2,nfft2);
NumUniquePts2 = ceil((nfft2+1)/2);
fftx2 = fftx2(1:NumUniquePts2);
mx2 = abs(fftx2);
mx2 = mx2/length(x2);
mx2 = mx2.^2;
if rem(nfft2, 2)   % Odd nfft excludes Nyquist
  mx2(2:end) = mx2(2:end)*2;
else
  mx2(2:end -1) = mx2(2:end -1)*2;
end
f2 = ((0:NumUniquePts2-1)*Fs/nfft2)*1000;
figure;
plot(f1,mx1);
title('Power Spectrum of H data');
xlabel('Frequency (mHz)');
ylabel('Power');
figure;
plot(f2,mx2);
title('Power Spectrum of D data');
xlabel('Frequency (mHz)');
ylabel('Power');
Div=mx1./mx2;
figure;
plot(f1,Div);
title('H/D Power Spectrum data');
xlabel('Frequency (mHz)');
ylabel('Power');
```

Appendix C

Text file sample of the data

```
DATA_TYPE        1-minute
SERIAL_NUM        5
STATION_NAME           HER
GEODETIC_LATITUDE     -34.340
GEODETIC_LONGITUDE    19.240
RECORD_TIME            2009/01/04,00:00:00
REPORTED         HDZF
SAMPLING_TIME          60
MAG_RANGE        1000
HEADER_DATA_NUM      288
HEADER_DATA_TIME 00:00:00
BIAS_H                 10359.51
BIAS_D                    21.48
BIAS_Z                 -22847.95
BIAS_F                 25086.26
HEADER_DATA_TIME 00:05:00
BIAS_H                 10359.51
BIAS_D                    21.48
BIAS_Z                 -22847.95
BIAS_F                 25086.26
CORRECT_NUM            11
CORRECT_INF            00:04:59,-70
CORRECT_INF            01:05:00,-360
CORRECT_INF            04:04:59,-50
CORRECT_INF            06:04:59,-50
CORRECT_INF            08:04:59,-190
CORRECT_INF            11:04:59,-100
CORRECT_INF            14:04:59,-120
CORRECT_INF            16:04:59,0
CORRECT_INF            17:04:59,-190
CORRECT_INF            21:04:59,-80
CORRECT_INF            23:04:59,-60
This storage format file was converted from Memory Card data by
using RtoStorageV1.m
The data reading program is ReadRSv1.m
The data writing program is WriteStorageV1.m
Storage Format Data Version 1
This storage format data was converted by using
StorageToStorage.m ver 1.02
Temperature Correction Factor [nT/deg] : -0.175300 -3.524200
1.050400
Temperature Averaging Interval [min] : 180
Offset value for each component : 0.000000 0.000000 0.000000
Amplitude Correction Factor : 1.032180 1.032180 1.032180
Cancel value at the date change : 0.000000 0.000000 0.000000
0.000000
__‘

'F™ÿ_@“?¸ÆÜKÊF__Û»_€5¼@¾¦A"'FõT@·?¸ÆåKÊF__Ù»_€5¼€º¦A__€O__€O__€O_
_€O__€¿__€¿__pÂ«'Fñ5ã?ü?¸ÆALÊF__Þ»_€5¼€ç¦Aè'F]ŠÕ?ö?¸ÆGLÊF__á»__5¼
```

€ç¦AŒ'F«?Ã?4@¸ÆmLÊF__×»__5¼Àã¦Aw'F6yœ?p@¸ÆŸLÊF__Û»__5¼ÀÔ¦A’'F_g€?
?@¸ÆÂLÊF__Õ»__5¼Àã¦Ax'Fp€o?Ò@¸ÆùLÊF__á»__5¼€ç¦Am
'F}M_?fA¸ÆHMÊF__ä»__5¼_à¦AI
'FÊ:Ø>ðA¸ÆŠMÊF__Ô»__5¼@Ü¦AÑ_'Fì]•>aB¸Æ£MÊF__á»__5¼€Ø¦A²
'FJjÎ=ÈB¸ÆÆMÊF__Õ»__5¼@Ü¦A_
'FÅÛ¼½iC¸Æ7NÊF__Õ»__5¼@Ù¦A©_'F_îÛ¾ÃC¸ÆtNÊF__Ù»__5¼_Ñ¦A~_'F_‡%¿\D¸
ÆöNÊF__Õ»__5¼€Ø¦AÆ_'F®
r¿§D¸ÆIOÊF__Ö»__5¼@Í¦Aà_'Fœpœ¿ÑD¸ÆuOÊF__å»__5¼@¾¦A·
'F?U©¿ðD¸Æ¾OÊF__Ø»__5¼ÀÅ¦A¶_'FÐ™´¿¤D¸ÆOÊF__à»_€4¼ÀÔ¦Ad
'FžûÇ¿sD¸Æ¤OÊF__Þ»_€4¼@Í¦Aä'FV“ï¿KD¸ÆšOÊF__Ý»__5¼€º¦Aì
'FNOù¿_D¸ÆqOÊF__Ó»__5¼ÀÅ¦A4
'Fm(_ÀdD¸Æ?OÊF__×»_€4¼@Í¦AK_'F_Ó_ÀÚD¸ÆÈOÊF__Ô»_€4¼€É¦A'
'FD~ À@E¸ÆéOÊF__Ø»_€4¼_Â¦A(_'FŠ<(À—E¸Æ_PÊF__Ñ»__5¼_³¦A6_'F
°2À©E¸Æ_PÊF__Í»_€4¼€É¦A__'Fài4À«E¸Æ_PÊF__É»_€4¼€É¦AÊ_'F??7ÀkE¸ÆÇO
ÊF__Õ»_€4¼_Ñ¦AŒ_'F¥ 6ÀûD¸ÆŠOÊF__Ö»_€4¼_Â¦A_ 'FÊJ5À°